Modeling the System Parameters of WASP12-b

Department of Astronomy, San Diego State University, 5500 Campanile Drive, San Diego, CA 92182-1221

May 9, 2015

ABSTRACT

WASP-12b is an interesting exoplanet discovered by Hebb et al. in 2009. Much has been published in the literature about this system, and it is imperative to obtain precise values of the system parameters. We use the Eclipsing Light Curve (ELC) code to simultaneously model five light curves and one set of radial velocity measurements of WASP12-b transits. We obtain fairly good fits to the data, and we compare our results to two previous results from the literature.

1. Introduction

WASP-12b is an extraordinary transiting Hot Jupiter discovered in 2009 by Hebb et al. It is the most irradiated planet to date, with an incident stellar flux of approximately 9×10^{9} erg cm^{-2} s^{-1} and an equilibrium temperature of 2516 ±36*K*. This high irradiation can be attributed to the short orbital period of ~ 1.09 days. Hebb et al. also measured the transit depth to be 14 mmag, which is a rather deep transit. There is also evidence that the planet may harbor traces of atmospheric water, although this claim is hotly disputed (Kreidberg et al, 2015). All of these characteristics make WASP-12b one of the most interesting extrasolar planets to study.

Maciejewski et al. obtained photometry for two transits of WASP12-b in February 2010. Using the JKTEBOP code (Southworth et al., 2004a,b), they derived the orbital parameters and found that they agreed with those measured by Hebb et al. (2009). Maciejewski et al. also found a TTV signal that seems to suggest the presence of another terrestrial planet in the system.

Because WASP-12b has become a testbed for irradiated atmospheres and tidal distortion models, it is of paramount important the orbital parameters of the system be measured precisely. In this report we model photometric and spectroscopic WASP-12b data using the ELC code (Orosz & Hauschildt 2000), and then compare our results with those obtained in the Maciejewski et al. manuscript.

2. Observations and Calibration

A partial WASP-12b transit was obtained in the I-band using the 40-inch reflector telescope at Mount Laguna Observatory (MLO) in San Diego, CA on 19 April 2015. These photometric data were obtained with 2048x2048 CCD that has a pixel scale of 0.41 ”/pixel and a field of view of 14’ x 14’. Ten dome flats were taken using a white screen illuminated by a projector, and bias frames were taken in the usual way. Because the CCD was cooled to -120 Celsius, dark frames were not considered. A total of 602 ten second exposures were taken, although ingress was not obtained due to limited observing time. It also important to note that the egress data show a large scatter due to increasing values of airmass.These photometric data were then calibrated in the standard way using the AstroImajeJ open source software package.Finally, these calibrated MLO data were normalized by the out-of-transit section of the light curve and then converted to magnitudes.

Figure 1 shows the sky brightness light curve for the I-band WASP-12b transit observed from MLO. The data set can be divided into three sections: the rapidly decreasing sky brightness to the left of the vertical dashed line, the approximately steady data between the two vertical lines, and the brightness ramp to the right of the vertical solid line. The data to the left of the vertical dashed line is of poor quality due to its high sky count, and the corresponding transit times are excluded from the sample. We attribute the brightness ramp to the right of the vertical solid line to increasing airmass.

Because a partial transit does not offer enough data to accurately model a light curve, we include several light curves from the literature. The R-band photometric data used in the Maciejewski et al. data are available online. Two additional R-band light curves and one I-band light curve were also obtained from the amateur website, Exoplanet Transit Database [1] (Poddany et al. 2010). Some of the data suffer from several observational defects, and most of the data do not include error bars. However, the website tags each data set with a Data Quailty (DQ) flag, where DQ = 1 is high quality data while DQ = 5 represents very poor data. Only data with error bars and that are of quality DQ $\leq$ 2 are included in this sample.

There are five light curves in total, three of which are in the R-band and two of which are in the I-band. The transit times for all five datasets were converted from UT-based JD into BJD based on Barycentric Dynamical Time using the on-line applet provided by Eastman et al.[2] (2010). Additionally, we use the sample of 21 radial velocity measurements from the 2009 discovery paper by Hebb et al as our spectroscopic sample.

---

[1] http://var2.astro.cz/ETD/

[2] http://astroutils.astronomy.ohio-state.edu/time

3. Modeling of Photometry and Spectroscopy

The Eclipsing Light Curve (ELC) code (Orosz & Hauschildt 2000) was used to model the system parameters of the WASP-12b system by simultaneously fitting all the photometric and spectroscopic.For computer efficiency, the code uses a "filter wheel" to model light curves for all eight of the Johnson UBVRIJHK filters at each phase in the orbit. The initial parameters are fed into the code through an input file. Also, the code includes a suite of local and global optimizers. For each of these models, the goodness of fit is determined using the standard chi-square statistic.

We model the WASP-12 system using the "model atmospheres" mode.In this mode, the host star is divided into a user-specified number of tiles, and the intensity of the stellar atmosphere is computed at each surface normal of the tile. The appropriate limb darkening law is used to calculate the intensity at all other angles. Because the host star is known to be a F95 star (Hebb et al., 2009), we include the appropriate limb darkening values from Claret & Bloemen (2011). Most of the initial input values are taken from either the Hebb et al. discovery paper or from the Maciejewski et al. manuscript. Additionally, we assume the eccentricity of the planetary orbit is zero (Campo et al. 2011; Husnoo et al. 2011; Croll et al. 2011).

We specify nine system parameters in our model: the inclination, orbital period, the time of conjuction, mass ratio, the ratio of the stellar radius divided by the planetary radius, the stellar radius, the primary mass, the orbital separation, and the radial velocity amplitude of the star. Note that the orbital separation cannot be determined from light curves or radial velocity measurements. We include the orbital separation simply as a derived parameter to be calculated by the ELC model. By directly comparing the orbital separation with previously derived values, we're setting a sanity check to ensure that the model is working correctly. Some of the primary ELC runs discussed in the next section used the stellar temperature as a sanity check, although the orbital separation was preferred for the final run. A genetic algorithm based on the pikaia routine developed by Charbonneau (1995) is used to explore the entire parameter space and determine the global x^2 of each of these system parameters.

Once the ELC run is finished, we use the JPlotterSuite developed by Justin Stevick to analyze the x^2 parameter space. In theory, a good model fit should form a parabola in the parameter space. The minimum of the parabola is defined to the x^2 value of the given parameter. To find the $\pm 1\sigma$ uncertainties, one would add one to the x^2 value and then move horizontally in both directions until the parabola is intersected. The x-axis values that intersect the parabola on either side of the x^2 value represent the $\pm 1\sigma$ uncertainties. The *chiPlotter* routine by Justin Stevick is used to plot these parameter space parabolas and calculate the $\pm 1\sigma$ uncertainties of each parameter.

3.1. Fitting Procedure

Although we've required the amateur light curves to have error bars, most of those error bars seem unrealistically large. In other words, the amateur light curves seem to contain exceedingly large scatter. We define the chi-square statistic to be

$$x^2 = \sum_{i=1}^{N} \left(\frac{y_i - \mu}{\sigma}\right)^2, \qquad (1)$$

where y_i is the datum, μ is the mean of the distribution, and σ is the standard deviation. The reduced x^2 is then defined to be x^2 / N, where N is the number of degrees of freedom subtracted from the number of data points. It's easy to see that if σ is exceedingly large, then the reduced $x^2 < 1$. and the model is overfittig the data. Our preliminary runs of the ELC code resulted in $x^2 < 1$ for each of the amateur light curves. One can also see that the errors bars are too large by simply plotting the amateur light curves, although this a less convincing argument than the quantitative argument given above. The egress section of the I-band light curve obtained from MLO also seems to overfit the data, most likely due to the large, systematic scatter present in the transit egress.

For each amateur light curve, the standard deviation of the uncertainty values was calculated. These calculated standard deviations became the adopted uncertainties for every data point in the respective file. Subsequent runs of the ELC code resulted in the reduced $x^2 \sim 1$ with these adopted uncertainties.

Several attempts were made at correcting the uncertainties of the MLO I-band dataIn theory, the transit egress should be a flat line while the full transit data should be continuously increasing or decreasing. We would therefore expect $x^2 = 1.0$ for any model of the transit egress. Our attempts at correcting the uncertainties focused on correcting the egress uncertainties, and then applying the same scaling law to the entire transit dataset. Our first attempt involved scaling the transit uncertainties by the reduced $\overline{x^2_{egress}}$. From (1),it's easy to see that the reduced $x^2 \sim 1$ if each egress uncertainty is scaled by the square root of the reduced chi-squareIn other words,

$$\sigma_{new} = \sigma_{old} * \sqrt{x^2_{reduced,\ egress}} \qquad (2)$$

Doing so, we scaled the transit data set by ~ 3.872 to obtain a final reduced $x^2 \sim 0.5$ during the subsequent ELC run. Our second attempt involved binning the egress data and repeating the same process. By binning the data, we hoped to constrain the scatter in the later half of the egress data. Each bin contained four data points, and we scaled each uncertainty by ~ 3.872. However the subsequent ELC run resulted in a reduced $x^2 \sim 0.74$, meaning the model was still overfitting the data. Our third attempt involved weighing each individual point by its airmass value at the time of observation. A Python code was written to search through the header of each image file, find the airmass value, and then scale each transit datum by its corresponding airmass valueThis method proved to be successful, and ELC returned a reduced $x^2 \sim 2.6$. We then applied a fourth method in hopes of obtaining a fit even closer to $x^2 = 1.0$. By eye we chose what we believed to

be the first egress datum, and found that its corresponding airmass was nearly equal to 2.0. We then binned the egress data into three sections. The first section contained all the airmass values between 2.0 < sec(x)<2.5, the second section contained the range 2.5 < sec(x)<3.0, and the third section contained all the egress data with airmass values larger than 3.0. Using this method, we obtained a reduced $x^2 \sim 2.13$.

4. Results and Discussion

We define the ELC run that obtained $x^2_{reduced} \sim 2.13$ to be our best fit, and all the results discussed in this section relate to that particular run. This fit was obtained using 100 population members spanning 1000 generations.

Table 1 shows the best fit values for the nine parameters, as well the corresponding values found in Maciejewski et al. and Hebb et al. We restate that the separation cannot be determined from the photometric and spectroscopic data alone. It is included in the parameter set simply as another parameter for ELC to match. Since the ELC orbital separation agrees with that of Hebb et al., we can feel more confident that the input file was made correctly and that our modeling of the observables can be trusted.

The orbital period, T_{conj}, inclination, mass ratio, primary mass, and orbital separation agree with those values reported by both Maciejewski et al. and Hebb et al., to within 1σ error bars. While the radii ratio, primary radius, and stellar reflex velocity values determined by ELC are not too distant from those in the literature, they are outside the bounds of the 1σ uncertainties.

Figure 2 shows the x^2 parameter space created by the chiPlotter routine. Some of the parameters are well-constrained by the data and form perfect parabolas, while other parameters appear to form slightly less perfect parabolas.This is expected for the separation parameter, as the orbital separation is a derived parameter that depends on various other observables and can therefore not be solved from the data alone. Figure 3 shows the inclination parameter space; it seems that the parameter space was not fully filled in by the 1000 generations. Overall however, by the sole basis of the chiPlotter output, the ELC model seems to fit the data fairly well.

Figures 5 - 8 show the photometric phase-folded data sets, with the ELC model light curves plotted on top. Overall, each of the model light curves fit the data pretty well. The reduced x^2 of each data set are as follows: 2.71 for the Maciejewski sample, 1.08 for the first Naves R-band sample, 1.04 for second Naves R-band sample,1.22 for the MLO sample, and 1.04 for the Shadic I-band sample. The Maciejewski et al. sample has the largest reduced x^2 of the five samples, and this seems to agree with the published results. Using the JKTEBOP code, Maciejewski et al. obtain a reduced $x^2 = 1.1373$ using the square-root limb darkening law, which they argue models their data better than the linear limb-darkening law or the logarithmic law. When doing so however, they obtain non-physical limb darkening coefficients.They get around this by keeping the second limb darkening coefficient fixed and allowing only the first coefficient to float.They obtain

physical results by doing so, but their reduced x^2 increases to 2.8660. Because we've used the "model atmospheres" version of ELC in this study, we do not fit for limb darkening at all. Instead, the limb darkening values for each filter remain fixed at the Claret & Bloeman values in the input file. It therefore seems reasonable that our Maciejewski et alsample agrees more with their second reduced x^2 than with their first result. Also recall that the uncertainties of the Maciejewski et al. sample have not been altered in any way.

Figure 9 shows the radial velocity model plotted on top of the Hebb et al. radial velocity values. The reduced $x^2 = 5.69$, which is much higher than the above values for the light curves. This is not surprising however, since the radial velocity values uncertainties were not altered in any way. Also, the Hebb et al. sample only consists of 21 points, which is a rather small sample size to fit for.

5. References

Campo, Ch.J., Harrington, J., Hardy, R.A., et al. 2010, ApJ, 727, 125

Chambers, J.E. 1999, MNRAS, 304, 793

Charbonneau, P., 1995, Genetic Algorithms in Astronomy and Astrophysics, The Astrophysical Journal (Supplements), 101, 309

Claret, A., & Bloemen, S. 2011, A&A, 529, A75

Eastman, J., Siverd, R., & Gaudi, B.S. 2010, PASP, 122, 935

Hebb, L., Collier-Cameron, A., Loeillet, B., et al. 2009, ApJ, 693, 1920

Husnoo, N., Pont, F., Hebrard, G., et al. 2010, MNRAS,413, 4

Kreidberg, L., et al. 2015, arXiv:1504.05586

Maciejewski, G., Errmann, R., Raetz, S., et al. 2011, A&A, 528, A65

Poddany, S., Brat, L., & Pejcha, O. 2010, New Astron., 15, 297

Orosz, J. A., & Hauschildt, P. H. 2000, A&A, 364, 265

Southworth, J. 2008, MNRAS, 386, 1644

Southworth, J. 2010, MNRAS, 408, 1689

Table 1. WASP-12b System Parameters

Paramter	Thomadis et al	Maciejewski et al	Hebb et al	Unit
Orbital Period	1.091422±0.00000036	1.09142275±0.000000033	1.091423±0.003	Days
T_{conj}	$4508.4264^{+0.00023}_{-0.00024}$	···	···	Days[a]
Inclination	$83.31388^{+0.45920}_{-0.48678}$	$82.5^{+0.4}_{-0.7}$	$83.1^{+1.4}_{-1.1}$	Degrees
Mass Ratio	$0.00094^{+0.00007}_{-0.00002}$	···	0.00099±0.00015	···
R_* / R_p	$8.579^{+0.0206}_{-0.0238}$	8.5126±0.00016	8.512±0.0002	···
M_*	$1.57^{+0.0541}_{-0.2802}$	···	1.35±0.14	M
R_*	$1.675^{+0.023}_{-0.106}$	1.9±0.1	1.79±0.09	R
Stellar Reflex Velocity	$0.212^{+0.0039}_{-0.0040}$	···	0.226±0.004	km s^{-1}
Orbital Separation	$5.082^{+0.0613}_{-0.3435}$	···	4.926±0.l72	R

[a]date with respect to BJD - 2,450,000

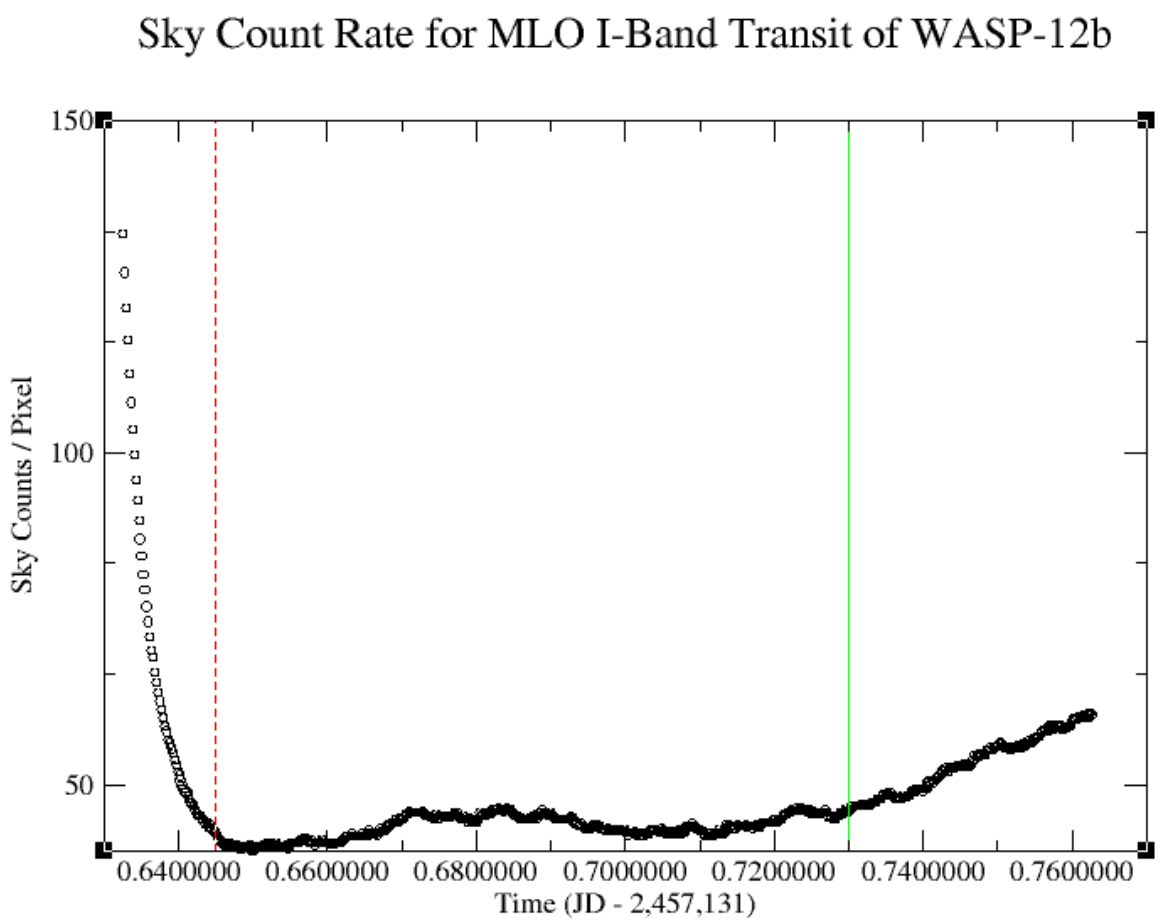

Figure 1. The sky brightness light curve for the I-band WASP-12b transit observed from MLO. The data to the left of the dashed line are of poor quality and are excluded from our sample. The data to the right of the solid line increase to sky noise due to increasing airmass.

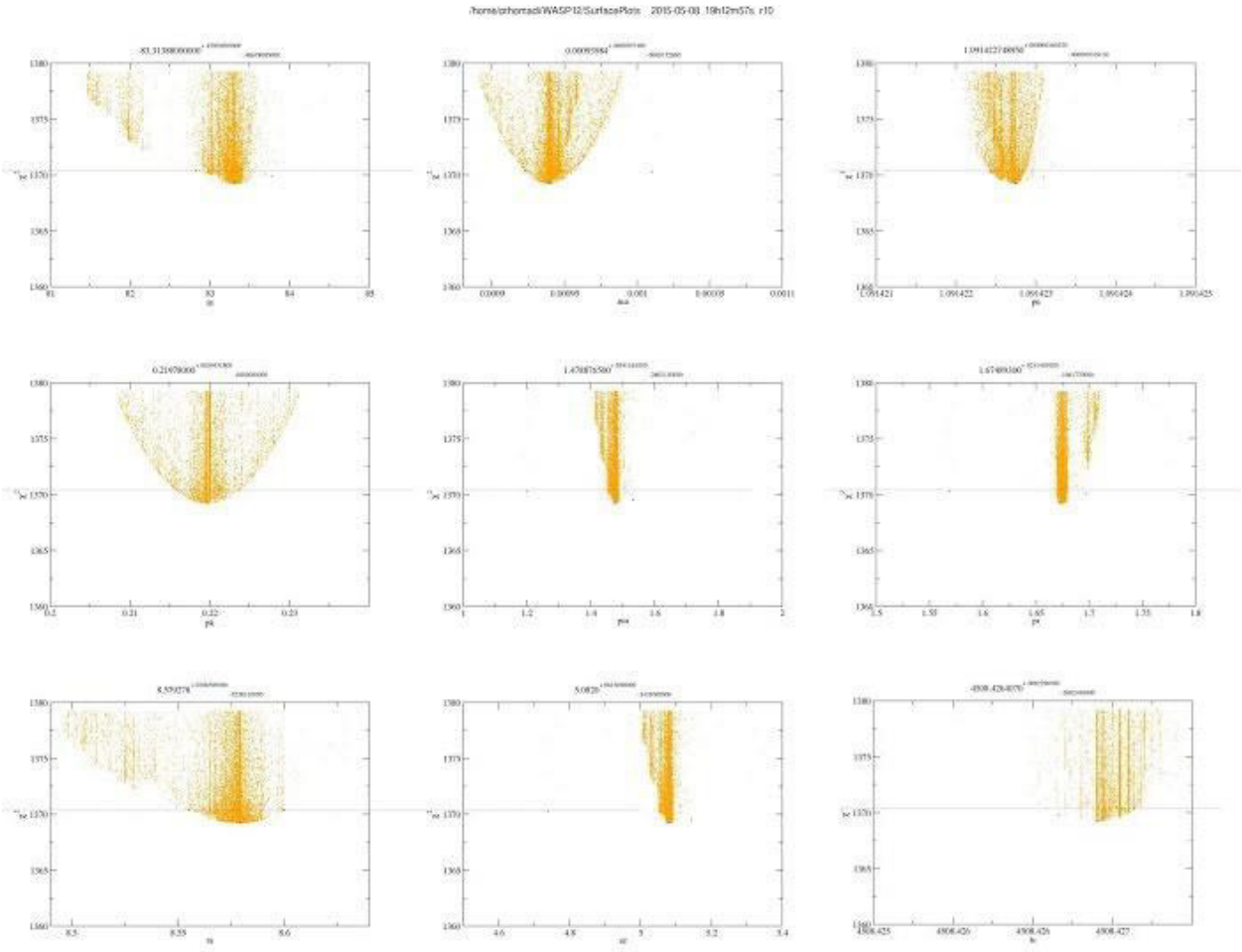

Figure 2. The χ^2 parameter space of each system parameter created by the *chiPlotter* routine All of the parameter spaces show clear parabolas, with the minimum value corresponding to the χ^2 statistic determined by the ELC genetic optimizer.

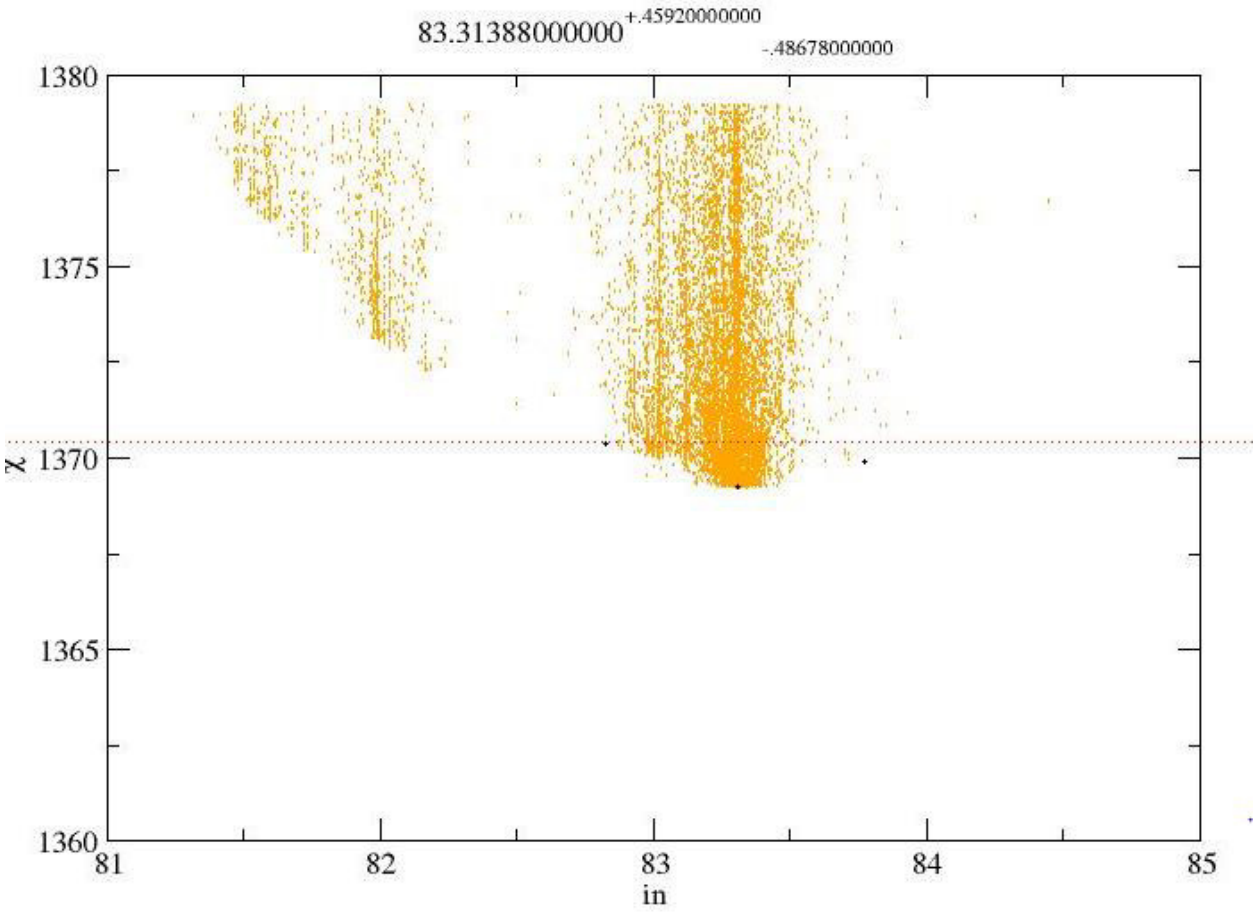

Figure 3. A zoomed-in image of the first panel from the montage. The χ^2 value and its associated uncertainties are plainly visible as black dots near the bottom of the parabola. Note that the upper-bound uncertainty seems to be offset slightly from the dashed horizontal line. This may be because the right side of the parabola seems to contain fewer points than the left side, under the horizontal line. Because of the fewer number of points, the *chiPlotter* routine cannot find a point on the right side that is equidistant from the center from the lower-bound uncertainty on the left side. This issue could be resolved by letting the genetic algorithm run for more generations.

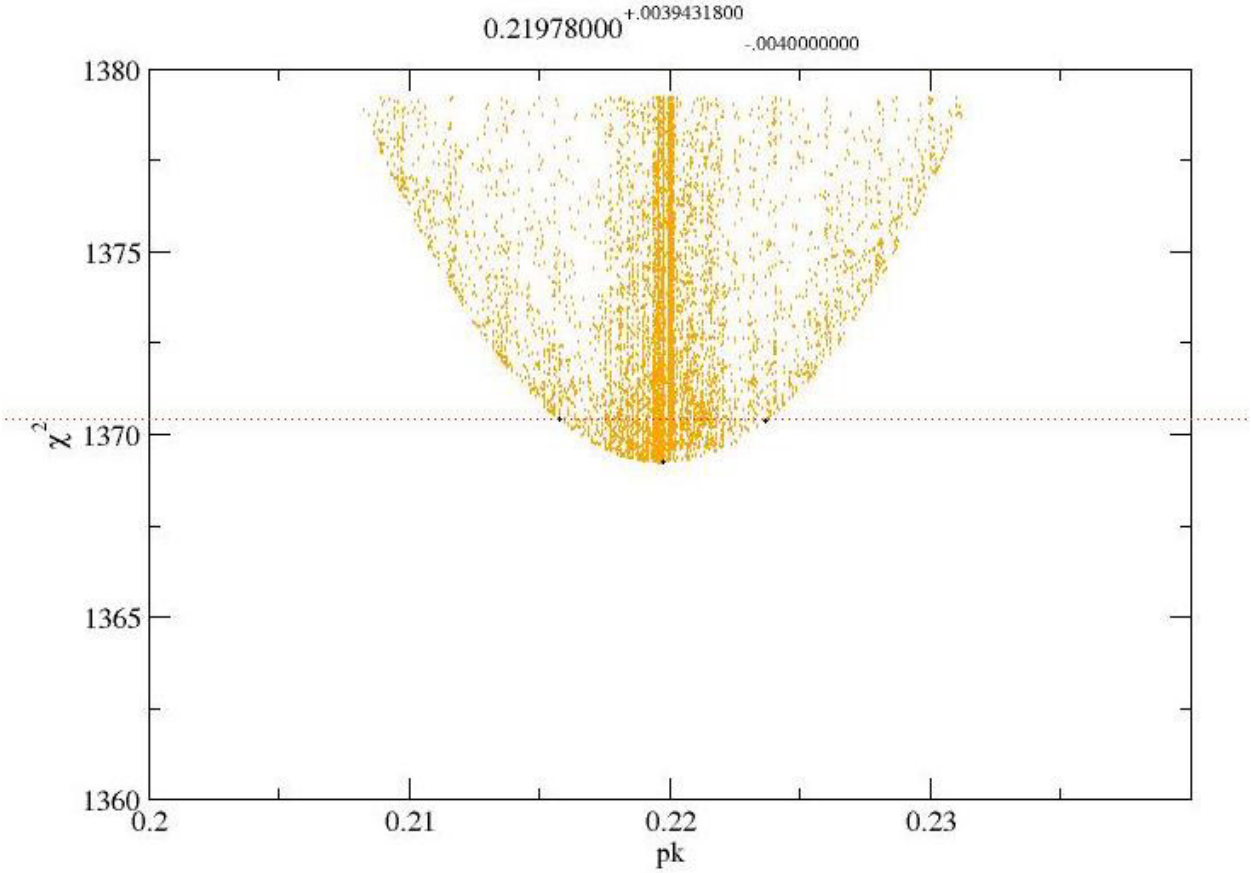

Figure 4. The parabola is clearly shown, and the ±1σ uncertainties are equidistant from the center. It seems that the stellar reflex velocity is well-constrained by the data.

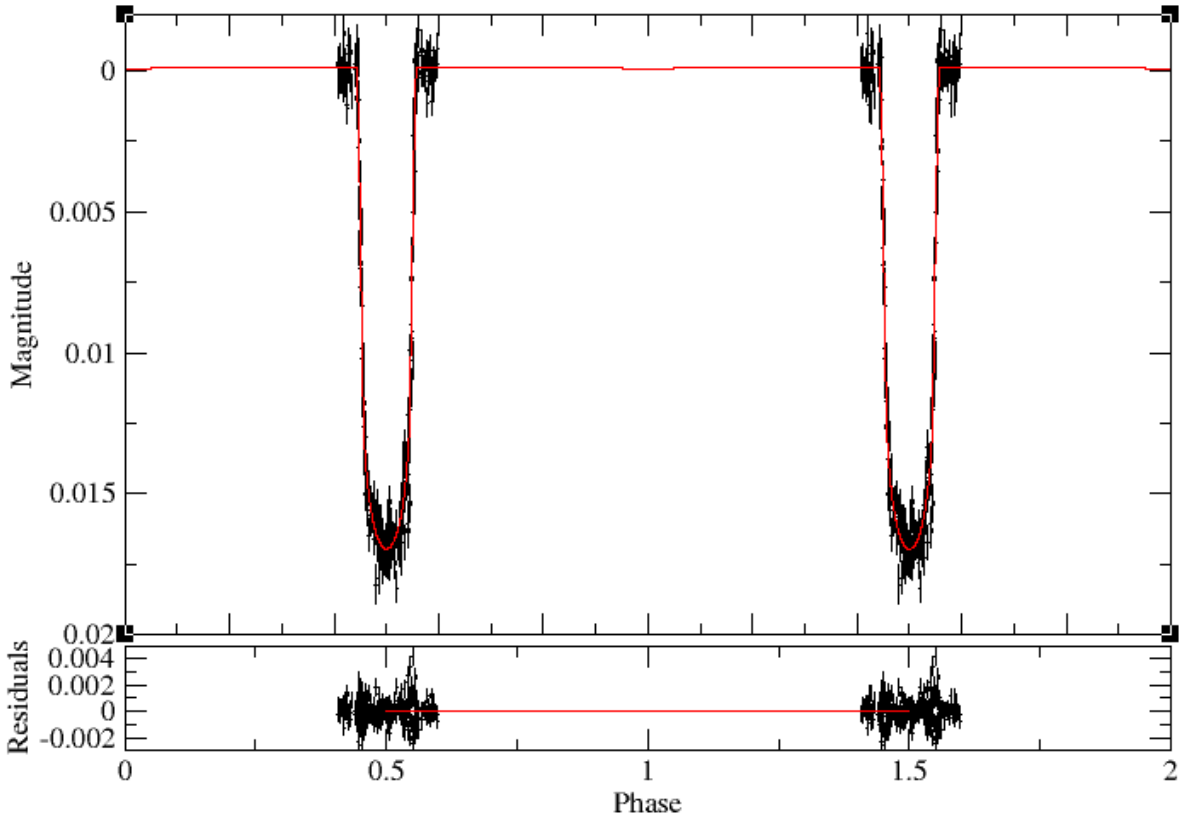

Figure 5. The ELC model of the R-band WASP-12b transits from the Maciejewski et al. manuscript. The upper panel shows a very good fit to the data, while the bottom panel shows the fit to be good to within one part in 1000. Note that the upper panel is showing the relative magnitude during transit.

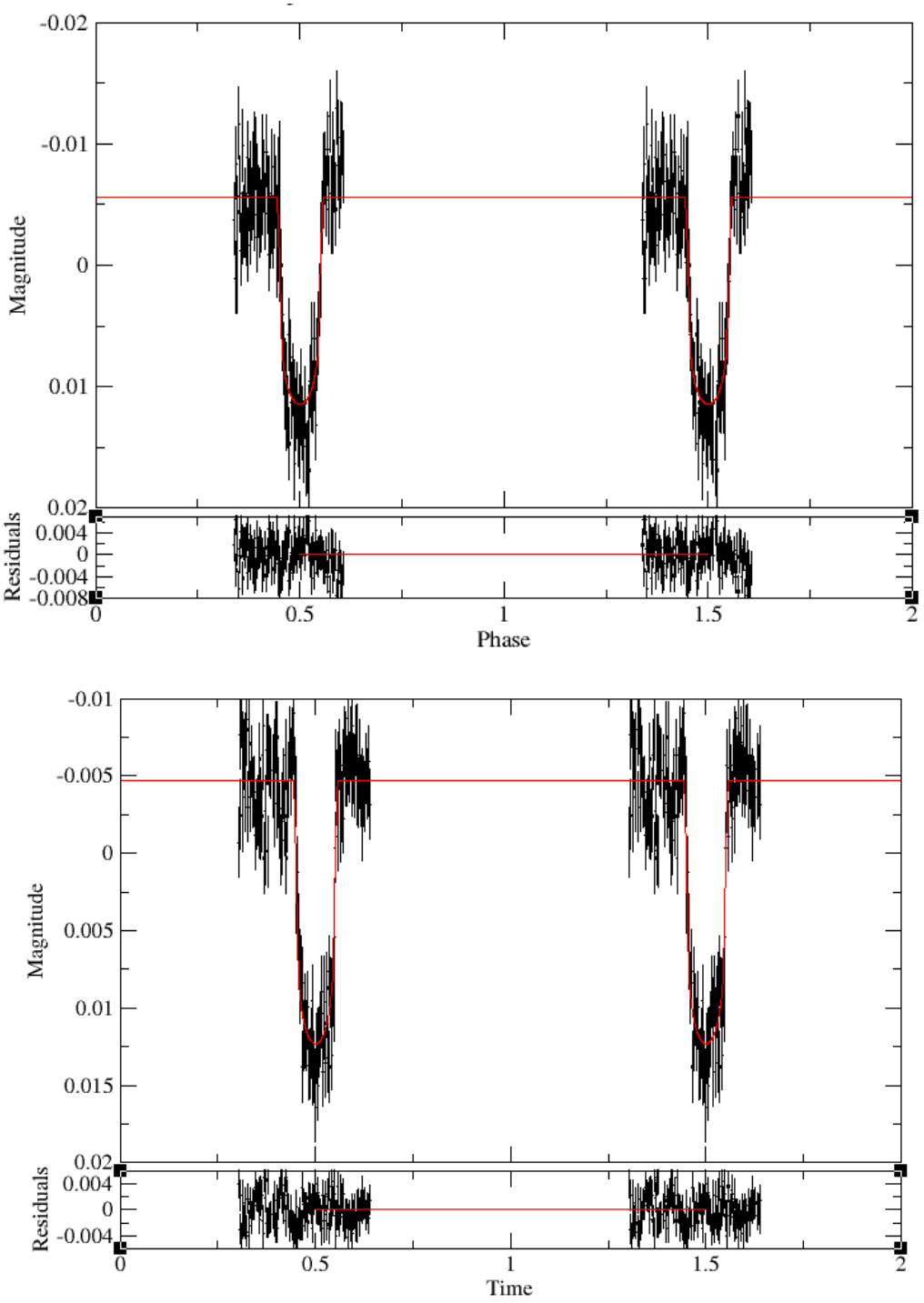

Figure 6. Upper Panel: The ELC model of the I-band WASP-12b transits from the Naves, R. amateur light curve from 2010-11-24. Lower Panel: The Naves, R. I-band transits from 2010-11-08. Note that the ELC model does indeed fit most of the data points towards the bottom of the transit, but the closeness of the fit is mainly obscured by the large error bars. These are the recalibrated error bars; the original uncertainties were much larger.

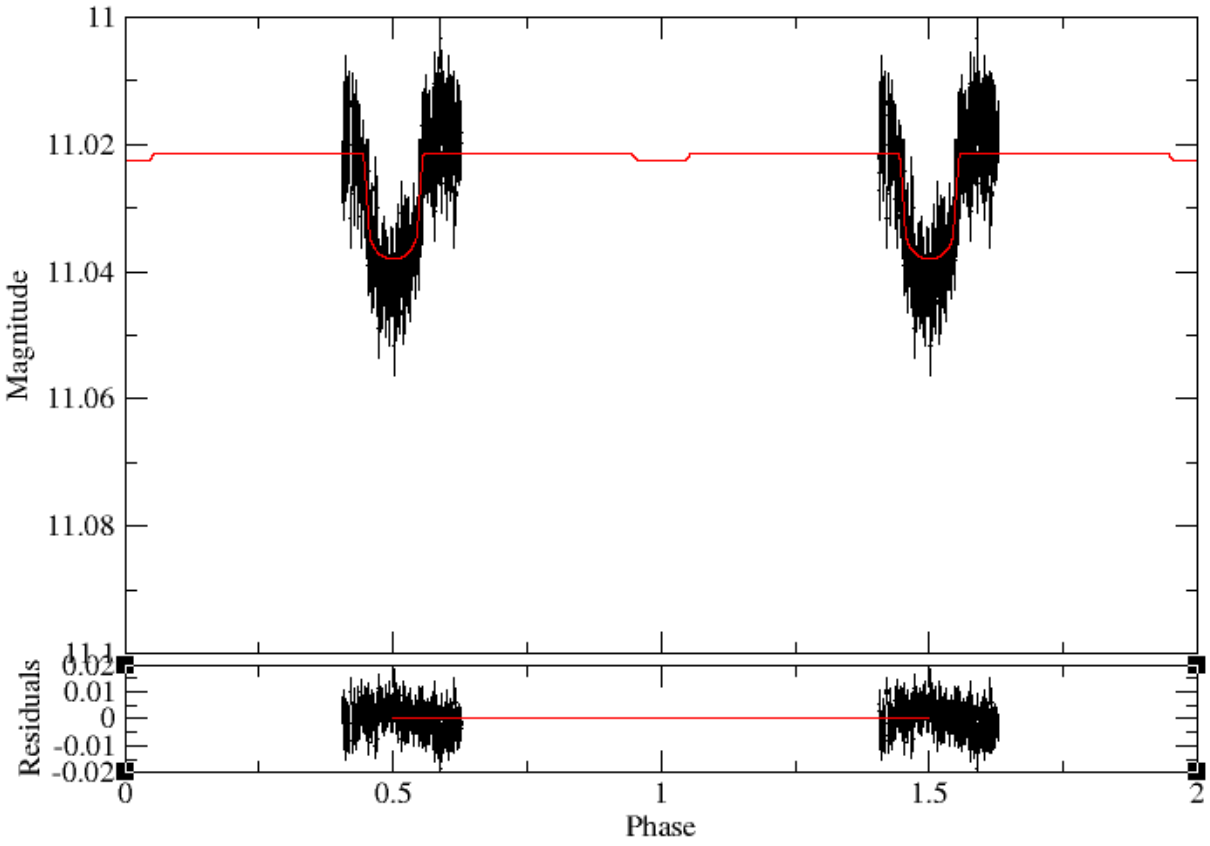

Figure 7. The ELC model of the I-band WASP-12b transits from the Shadic, S. amateur light curve from 2012-01-26. The lower panel shows the fit to be good to one part in a hundred, which is higher than the previous light curves shown. Also note the visible occultation in the center or the plot, which is not as visible in the previous R-band plots. This is not surprising of course, as occultation depth increases with increasing wavelength.

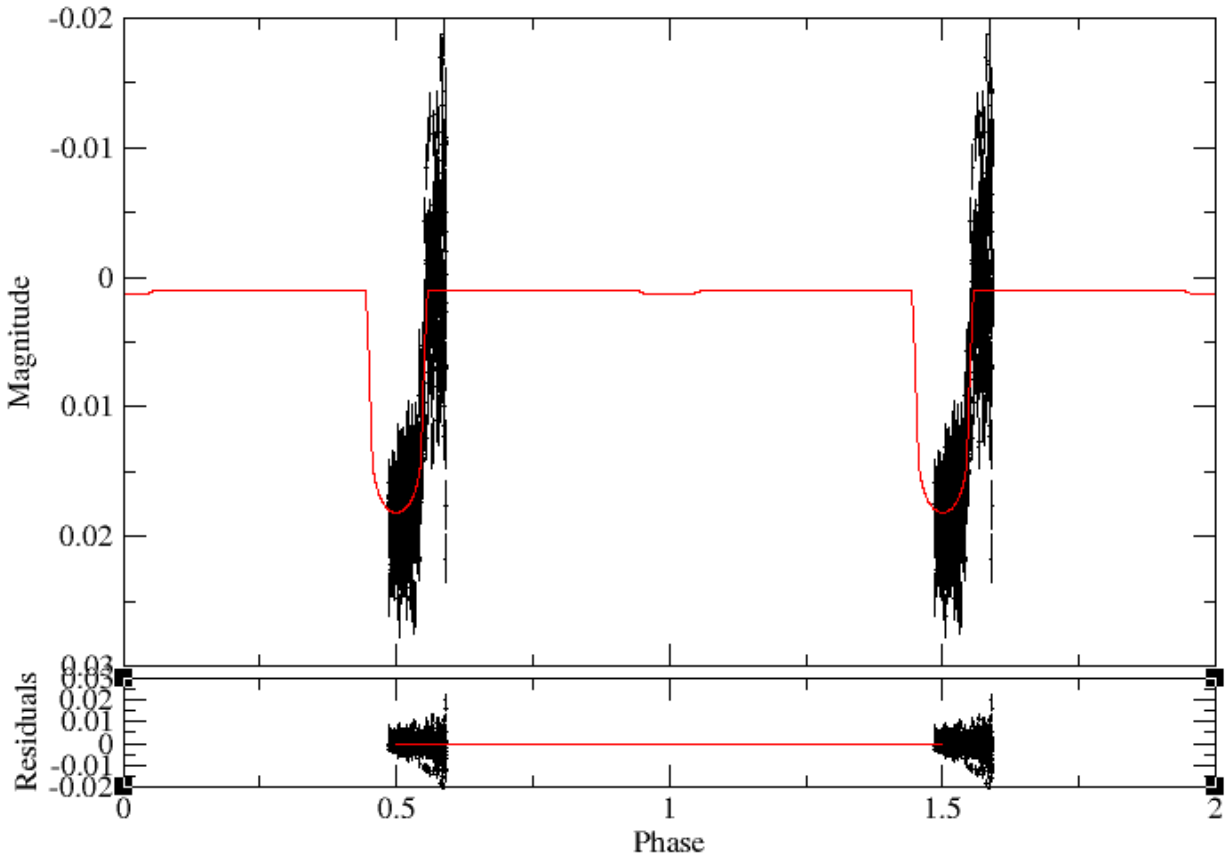

Figure 8. The phase-folded ELC model of the two I-band WASP-12b transits observed from MLO. Note that the ingress was not observed at MLO, hence the need for additional light curves. Also note the large scatter at egress.

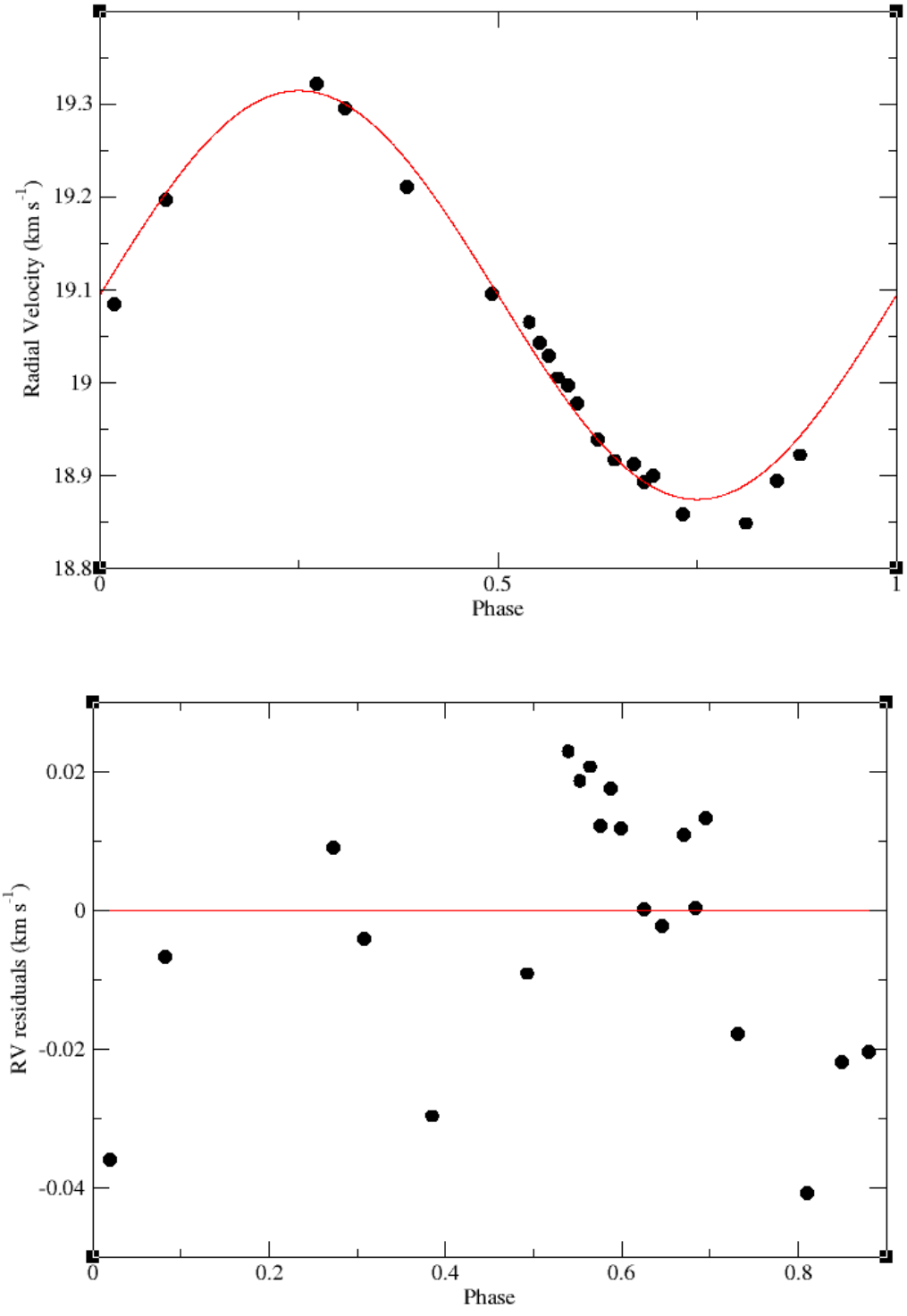

Figure 9. Top: The Hebb et al. radial velocity values are shown as black circles and the ELC model fit is plotted on top as a red line. Bottom: A residual plot the of the radial velocity curve. The plot shows that the fit is good to a couple parts per hundred, which is a factor of ten larger than most of the light curves.